

Two dimensional Ising model with long-range competing interactions

Sergio A. Cannas,^{*} Pablo M. Gleiser,[†] and Francisco A. Tamarit[‡]

*Facultad de Matemática, Astronomía y Física,
Universidad Nacional de Córdoba,
Ciudad Universitaria, 5000 Córdoba, Argentina[§]*

(Dated: March 23, 2022)

The two-dimensional Ising model with competing short range ferromagnetic interactions and long range antiferromagnetic interactions is perhaps the most simple one containing the minimal microscopic ingredients necessary for an appropriate description of the macroscopic properties of ultrathin films and quasi-two-dimensional magnetic materials. Despite such relative simplicity, the frustration introduced by the competition between interactions generates complex behaviors that have eluded, up to now, a complete understanding of its general properties. In this work we review recent advances in the understanding of both equilibrium and non-equilibrium properties of the model. This includes a detailed description of several known properties of the thermodynamical phase diagram, as well as the existence of several types of metastable states and their influence in the low temperature dynamics.

PACS numbers: 05.50.+q, 75.40.Gb, 75.40.Mg

I. INTRODUCTION

The Ising model with arbitrary interactions is perhaps the most successful one in statistical physics. Despite its (relative) simplicity, it has been used to model such a variety of complex systems exhibiting cooperative phenomena that it can be regarded with fairness as a paradigm of a model system. Besides its multiple applications in theoretical physics (in fact, Onsager's solution of the two-dimensional model was the cornerstone of the modern theory of critical phenomena) one of its most conspicuous application in condensed matter (and its original motivation) is related to the description of anisotropic magnetic materials. While mostly applied in the past decades to bulk magnetic materials, the advances in film growth techniques, such as atomic or molecular epitaxy, has raised a renewed interest in the behavior of the two-dimensional version of the model. In particular, the study of thin magnetic films and quasi two-dimensional magnetic materials (like the rare earth layers that occur in perovskite structures of $\text{REBa}_2\text{Cu}_3\text{O}_{7-\delta}$, RE being a rare earth of the lanthanide series [3]) has experimented an increasing interest during the last years. Part of this interest is obviously motivated by the great amount of applications they find nowadays in many different technological fields, such as data storage, catalysis and electronic uses are only a few examples, among many others. Nevertheless, they have also caught the attention of both theoretical and experimental physicists due to the rich insight they provide into the fundamental role that microscopic interactions play in determining the macroscopic properties of a material. One of the most interesting applications of the two-dimensional Ising model is related to the theoretical description of ultra-thin magnetic films, like metal films on metal substrates (e.g. Fe on Cu [1], Co on Au [2], see also [3] for a recent review on the topic). If the magnetic film is thin enough (less than approximately five monolayers) the atomic magnetic moments tend to align out of the plane defined by the proper film. This occurs because the surface anisotropy overcomes the anisotropy of the dipolar interactions, which favor in-plane ordering. Under these circumstances, one can then model the local magnetic momenta of the material by using Ising variables.

Any realistic theoretical description of a magnetic thin film must include, besides the usual short-range exchange interactions, also the long-range antiferromagnetic dipolar interactions. It is worth mentioning that dipolar interactions have been usually neglected, specially in thermodynamical studies, due to the small magnitude of dipolar interactions relative to the magnitude of the exchange interactions. Nevertheless, it is a well established fact that dipolar interactions can give place to very rich phenomenological scenarios, concerning both thermodynamical and nonequilibrium properties. In particular, when both interactions are present, the system is inherently frustrated, and many of the interesting static and dynamical properties of systems with dipolar interactions result, precisely, from this property.

^{*}Electronic address: cannas@famaf.unc.edu.ar

[†]Electronic address: gleiser@tero.fis.uncor.edu

[‡]Electronic address: tamarit@famaf.unc.edu.ar

[§]Member of CONICET, Argentina

In this paper we will review the recent advances in the study of equilibrium (*i.e.*, *thermodynamical*) and out of equilibrium properties of the Ising model with competition between short-range ferromagnetic exchange interactions and long-range antiferromagnetic dipolar interactions defined on a square lattice and ruled by the following dimensionless Hamiltonian:

$$\mathcal{H} = -\delta \sum_{\langle i,j \rangle} \sigma_i \sigma_j + \sum_{(i,j)} \frac{\sigma_i \sigma_j}{r_{ij}^3} \quad (1)$$

where $\sigma = \pm 1$ and δ stands for the quotient between the exchange J_0 and the dipolar J_d interactions parameters, *i.e.*, $\delta = J_0/J_d$. The first sum runs over all pairs of nearest neighbor spins and the second one over all distinct pairs of spins of the lattice. r_{ij} is the distance, measured in crystal units, between sites i and j . The energy is measured in units of J_d , which is assumed to be always positive (antiferromagnetic); hence $\delta > 0$ means ferromagnetic exchange couplings.

II. THERMODYNAMICAL PROPERTIES

A. Ground state

The basic features of the finite temperature phase diagram associated with Hamiltonian (1) were first derived by MacIsaac and coauthors in 1995 [4]. In that work the existence of equilibrium striped states was firmly established for the first time. They showed that the ground state of Hamiltonian (1) is indeed the striped one, provided that the relative strength of the interactions δ exceeds some positive value $\delta_a \approx 0.425$ [5]. If $\delta < \delta_a$ the ground state is the antiferromagnetic one. If $\delta > \delta_a$ the ground state is composed by antialigned stripes of width h , which depends on δ . MacIsaac and coworkers showed that for every finite value of $\delta > \delta_a$ there exists always a value of h such that the corresponding striped state has less energy than both the ferromagnetic and the checkerboard states, which had been previously proposed as the ground state for this system [6]. Moreover, they showed that this is true for *any* value of δ . In other words, the presence of the dipolar interactions, even with an infinitesimal strength, suppress the ferromagnetic ordering, favoring the formation of stripe domains. They also showed that for large values of δ the equilibrium width increases exponentially $h \sim e^{\delta/2}$. Although not rigorously demonstrated up to now, a very large amount of numerical evidence supports the results of MacIsaac and coauthors.

B. Monte Carlo finite temperature simulations

Most of the knowledge about the finite temperature equilibrium properties of the model has been obtained by means of Monte Carlo numerical simulations on finite lattices. These have been performed on square lattices of $N = L \times L$ sites [4, 7, 8, 9] using Metropolis or heat bath algorithms. Monte carlo simulations has been vastly used to study finite temperature properties of magnetic lattice spin models. However, performing Monte Carlo simulations in system (1) involves some particular subtleties to take into account, due to the presence of dipolar interactions.

First of all, the modulated nature of the ground state implies that the linear size L of the system must be chosen commensurate with the period of the modulation associated with the particular value of δ under consideration; otherwise, an artificial frustration is introduced.

A second point concerns the structure of the ground state as the value of δ is increased. For relatively large values of δ , striped states of widths similar to that of the ground state have very low energies. This may generate (as we will see later) multiple metastable states at low temperature, making it very difficult to equilibrate and therefore to determine the truly thermodynamically stable state.

Other complications arise as direct consequences of the long-range character of the dipolar interactions. Since every spin in the lattice interacts with each other, flipping a spin does not affect only a few neighbor spins, but *all* the rest of the spins in the lattice. This means that most of the powerful algorithms developed in the last years to improve the efficiency of Monte Carlo simulations (like block algorithms) do not apply, since most of them rely on the finite range of the interactions. To further complicate the situation, the antiferromagnetic nature of the dipolar term does not allow the application of some specially designed algorithm for systems with long-range ferromagnetic interaction [11]. This means that, except from some recent works on the triangular lattice[10], most of the simulations of this model are based on simple Metropolis or heat bath algorithms, in which the typical number of operations to perform a Monte carlo step goes as N^2 rather than N , as in systems with short range interactions.

Other consequences of the long-range character of the dipolar interactions are the strong finite-size effects, since in this case every spin feels *directly* the influence of the border. As in any type of system, the best way to diminish

border effects is to use periodic boundary conditions. While both the interpretation and implementation of periodic boundary conditions are straightforward in systems with short range microscopic interactions, their usage in systems with long-range interactions is more subtle. In a general situation, there are two alternative representations of a finite two-dimensional system with periodic boundary conditions. On one hand, we can visualize the system as a torus, where a given spin interacts with its closer neighbors defined by the topology of the torus, up to a certain range of interaction, that is, to consider a finite translationally invariant system. On the other hand, we can think that we have an infinite system, where the original finite system has been replicated infinite times in all the coordinate directions. In other words, we can think that the infinite lattice has been partitioned into cells of size $N = L^2$ and that we have chosen only the periodic solutions of the problem, with periodicity L in all the coordinate directions. While the difference between both views is just a matter of interpretation for systems with short-range interactions, the situation changes for long-range interacting systems. According to the second scheme, a given spin will interact with *infinite replicas of everyone of the rest of the spins* and we can express the effective interaction between two spins inside the system as an infinite sum over replicas (this includes a “self-interaction” term, that accounts for the interaction of every spin with its own replicas). On the other hand, in the closed topology of the first scheme it is consistent to consider that every pair of spins inside the system interacts only through its *minimal* distance over the torus. This corresponds to the minimal truncation of the infinite series of the previous scheme and it is sometimes called the *first image convention*. While the efficiency of both type of schemes can be very different in systems that presents low temperature ferromagnetic ordering, in the case of Hamiltonian (1) the differences are minimal [12], with a little improvement obtained with the first scheme. The usage of a particular scheme is then a matter of convenience. However, while the usage of the second scheme is straightforward, the implementation of the first is more involved, since the infinite series for the effective interactions are slowly convergent. The usual way of handling them numerically is to adapt the Ewald sums technique [3, 13], originally derived for systems of interacting charged particles [14, 15].

C. Low temperature equilibrium properties: metastable striped states

The finite temperature phase diagram in the (δ, T) space was first calculated using Monte Carlo simulations on small lattices ($L = 16$) by MacIsaac and coauthors in [4]. Further improvements at low temperature were obtained by Gleiser and coauthors in [8]. The numerical simulations showed that both the antiferromagnetic and the different striped states remain stable at finite temperatures below some δ -dependent critical temperature $T_c(\delta)$. At $T = T_c(\delta)$ the specific heat

$$C_L = \frac{1}{NT^2} \left(\langle H^2 \rangle - \langle H \rangle^2 \right) \quad (2)$$

presents a peak, indicating that the system undergoes a phase transition into a disordered phase. Both the nature of the disordered phase, as well as the order of the phase transition present several subtleties and will be considered in section IID. We will consider now the properties of the system at temperatures well below the critical one. We will concentrate our attention in the low δ region of the phase diagram, that is, where the first striped states emerge after the antiferromagnetic one, when the value of δ crosses $\delta_a = 0.425$. The transition points between the different striped states at $T = 0$ can be estimated by a numerical calculation of the striped states energies as a function of δ in finite size lattices of increasing linear sizes L [4]. We will denote by hi the striped state of width $h = i$, with $i = 1, 2, \dots$. The state hi in a translationally invariant lattice has a degeneracy $4i$, due to parallel translations along a coordinate axis and to $\pi/2$ rotations of the stripe pattern. Let $\delta_{i,i+1}$ be the transition point between the striped states hi and $hi + 1$. We have for the first striped states that $\delta_{1,2} \approx 1.26$, $\delta_{2,3} \approx 2.2$ and $\delta_{3,4} \approx 2.8$.

We now consider the transition between the striped states $h1$ and $h2$ at finite temperatures [8]. The different striped phases can be characterized by the order parameter:

$$m_h \equiv \frac{1}{N} \sum_{x=1}^N \sum_{y=1}^N (-1)^{f_h(x)} \sigma_{xy} \quad (3)$$

where the function $f_h(x) \equiv (x - \text{mod}(x, h))/h$ takes odd and even values with periodicity h [3]; m_h measures the overlap of the spin configuration with a vertical stripe pattern of width h . The thermodynamical averages $M_h = \langle m_h \rangle$ and its associated susceptibilities

$$\chi_h \equiv \langle m_h^2 \rangle - M_h^2 \quad (4)$$

can be calculated through Monte Carlo simulations. The stability of the striped phases can be analyzed by heating the

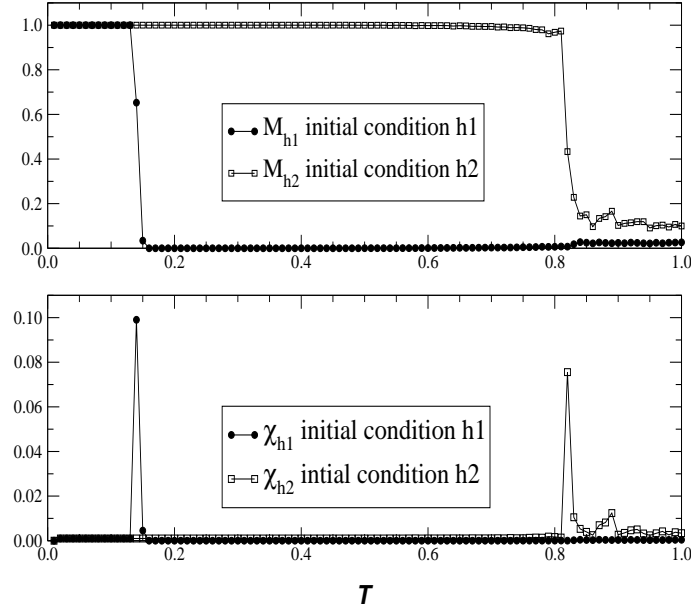


FIG. 1: Order parameters (3) and associated susceptibilities (4) *vs.* T when the system is heated starting at $T = 0$ from an initial (vertical) stripe configuration for $L = 24$ and $\delta = 2$; open squares: M_{h2} for an initial configuration h2; full circles: M_{h1} for an initial configuration h1.

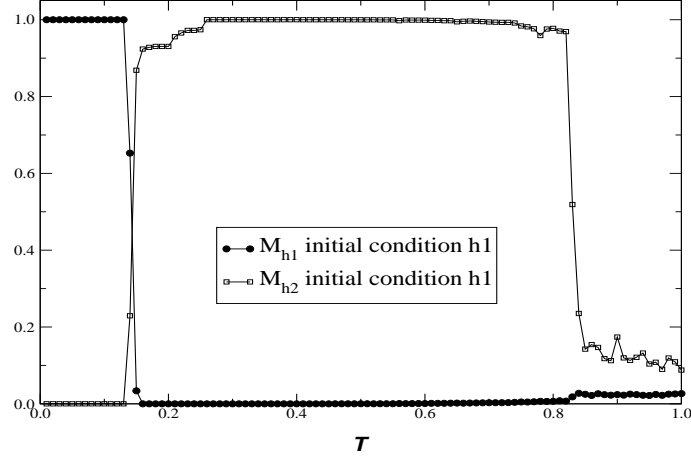


FIG. 2: M_{h1} and M_{h2} when the system is heated starting at $T = 0$ from an initial (vertical) stripe configuration for $L = 24$ and $\delta = 2$.

system from zero temperature, that is, by performing equilibrium Monte Carlo simulations in a sequence of increasing temperature values starting from $T = 0$, where the initial spin configuration at every temperature is taken as the last configuration of the previous one. The simulations start at $T = 0$ from an ordered configuration. In Fig.1 we show an example for $\delta = 2$, corresponding to an h2 ground state. In this case two simulations were performed in parallel, one starting from the h1 and the other from the h2 (vertical) striped states, and in each case M_{h1} and M_{h2} were respectively measured, as well as the corresponding susceptibilities. In Fig.2 we show a simultaneous measurement of M_{h1} and M_{h2} in a simulation started from the h1 state. When starting from h2 the system remains in this state up to the critical temperature (i.e., that of the peak in the specific heat) where M_{h2} suddenly drops to a small value, with an associated peak in the corresponding susceptibility. The same behavior is reversely obtained by slowly cooling the system from high temperatures. This shows that the h2 state is thermodynamically stable. On the other hand, when starting the simulation from the h1 state it remains stable up to certain temperature below the critical one, where it destabilizes and the h2 pattern emerges (see Fig.2), showing the metastable nature of the h1 phase for this

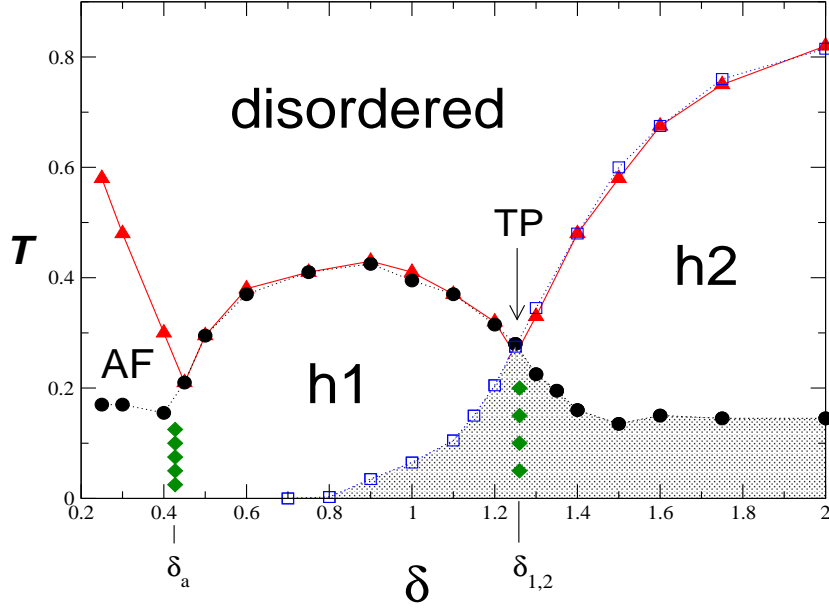


FIG. 3: (T, δ) phase diagram for low values of δ obtained from Monte Carlo simulations in $L = 24$ lattices. Triangles: critical temperature obtained from the maximum in the specific heat; circles: stability line of the h1 striped phase; open squares: stability line of the h2 striped phase; diamonds: first order transition lines between low temperature ordered phases. TP indicates a triple point.

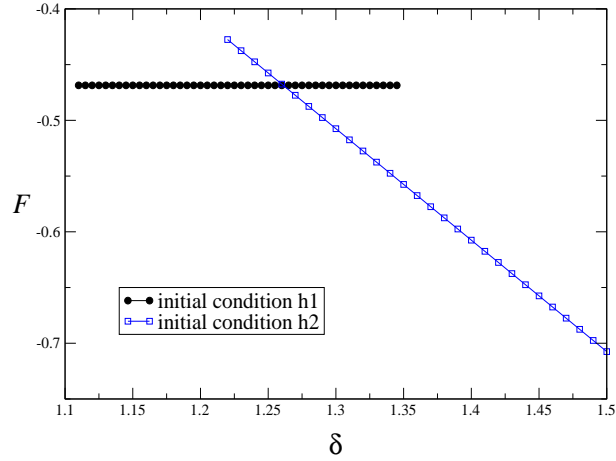


FIG. 4: Free energy per spin of states h1 and h2 *vs.* δ for $T = 0.2$ and $L = 24$.

particular value of δ . The reverse behavior is observed in the region $\delta < \delta_{1,2}$, where the h2 phase appears metastable down to a certain value $\delta \sim 0.7$. Repeating this procedure allows the calculation [8] of the stability lines for the h1 and h2 phases as a function of δ . The results are shown in the phase diagram of Fig.3. The coexistence of different states indicates that the transition between both ordered phases at low temperature is of the first order type. The first order transition line can be located by calculating the free energy per spin of each phase, which can be obtained by numerical integration

$$F(T, \delta) = U - T \int_0^T \frac{C(T')}{T'} dT' \quad (5)$$

where $U \equiv \langle H \rangle / N$ and $C(T)$ is obtained by heating from $T = 0$ up to the reference temperature T for every value of δ . For a given value of T , $F(T, \delta)$ is computed for different values of δ in each phase. The transition point is

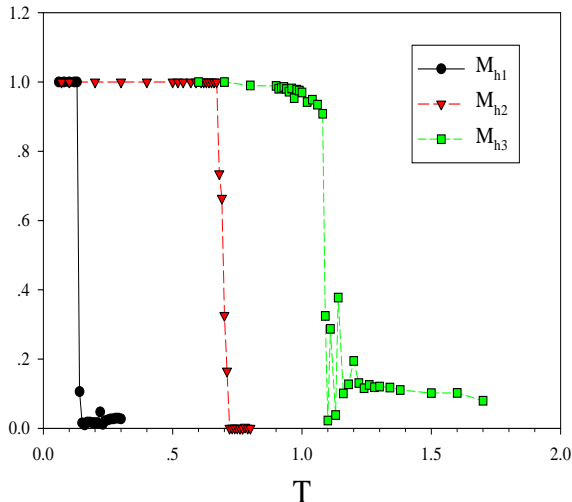


FIG. 5: Order parameters (3) *vs.* T when the system is heated starting at $T = 0$ from an initial (vertical) stripe configuration for $L = 24$ and $\delta = 2.6$; circles: M_{h1} for an initial configuration h1; triangle: M_{h2} for an initial configuration h2; squares: M_{h3} for an initial configuration h3.

calculated as the crossing point of the two curves, as depicted in the example presente in Fig. 4. The first order transition line between h1 and h2 phases is shown in diamonds in Fig.3. Following the same procedure another first order vertical line is encountered between the antiferromagnetic and the h1 phases [16]. Other vertical transition lines appear between ordered phases of higher h values [4].

We now turn our attention to the general features of the phase diagram shown in Fig. 3. We see that the first order line between phases h1 and h2 joins the point where the two stability lines cross, marked as TP in Fig. 3. Above the point TP both stability lines coincide with the maxima in the specific heat and thus with the transition lines to the disordered phase. As we will see in IID, those transitions are also of the first order type and, therefore, TP is actually a *triple point*. Below the triple point we have a metastability region, which appears shadowed in Fig.3. The corresponding spinodal lines are given by the continuation of the order-disorder transition lines below TP. Further evidence of the metastable nature of h1 and h2 phases in that region can be obtained by analyzing the relaxation of mixed states in the shadow region of the phase diagram [8]. Following the same procedures described above, the coexistence of striped states with larger values of h at higher values of δ can be verified. Notice that the spinodal line of h1 in the h2 region decays very slowly as δ increases; actually, it continues almost horizontal for a wide range of values of δ . Below this line the coexistence of multiple striped states can be found, for instance, between h1, h2 and h3 when $\delta_{2,3} < \delta < \delta_{3,4}$, as can be appreciated in the example for $\delta = 2.6$ shown in Fig.5. Coexistence of a larger number of striped states can be expected for higher values of δ . Moreover, other type of stable or metastable configurations (like mixtures of stripes of different widths) can also be expected in that region, as observed in a related three-dimensional model with competing nearest neighbors ferromagnetic interactions and long-range antiferromagnetic Coulomb-like interactions [22]. As we will see in III, the existence of metastable states has profound consequences in the far-from-equilibrium, low temperature properties of this system.

D. High temperature properties

When we increase the temperature the ordered phases undergo a phase transition into a disordered state. Booth and coauthors [7] showed that above and near the transition temperature the disordered phase is not paramagnetic, but instead it consist of extended ferromagnetic domains characterized by predominantly square corners (see Fig.6). This phase presents a fourfold rotational symmetry, as can be observed in numerical calculations of the structure factor

$$S(\vec{k}) = \left\langle \left| \sum_{\vec{r}} \sigma_{\vec{r}} e^{i\vec{k} \cdot \vec{r}} \right|^2 \right\rangle$$

which displays four symmetric peaks along the principal axes of the Brillouin zone [3]. As temperature is further

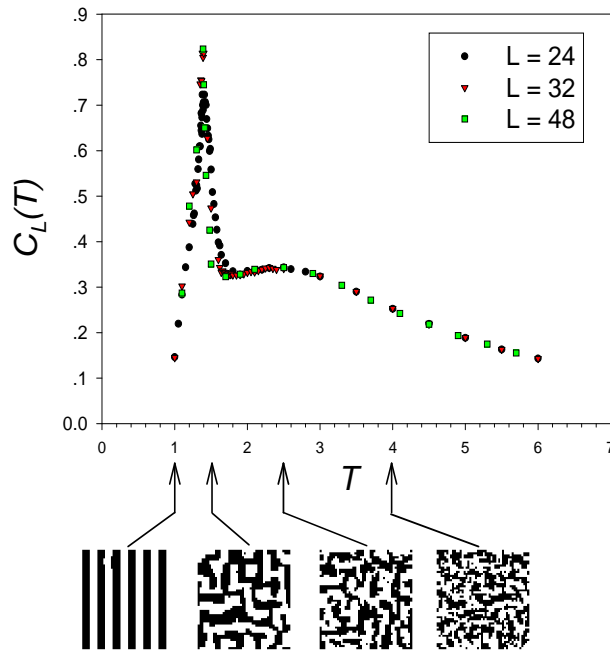


FIG. 6: Specific heat *vs.* T for $\delta = 3$ (corresponding to an h4 ground state) and different system sizes. Some typical equilibrium configurations at the indicated temperatures for $L = 48$ are shown below. Note the sequence of transitions h4 \rightarrow tetragonal \rightarrow paramagnetic.

increased, the four peaks become gradually smeared into a circle shaped crown, signaling the continuous replacement of the fourfold symmetry by the full rotational symmetry of the paramagnetic phase. Booth and coauthors proposed that the transition from the striped to this *tetragonal* phase can be characterized as an order-disorder one, associated to the loss of orientational order of the striped phase [7]. To characterize this symmetry breaking they introduced an order parameter

$$m \equiv \frac{n_v - n_h}{n_v + n_h} \quad (6)$$

where n_v (n_h) is the number of vertical (horizontal) bonds between spins that are antiparallel [7]. The absolute value of this order parameter is one in *any* stripe configuration and equals zero in any configuration with fourfold rotational symmetry. The numerical simulations performed by Booth and coauthors of $\langle m \rangle$ for values of $\delta \geq 3$ appeared consistent with a second order stripe-tetragonal phase transition [7]. In the same parameters region, the presence of the tetragonal phase shows its signature in the shape of the specific heat curve, as is illustrated in the example shown in Fig. 6, for $\delta = 3$. We see that the curve presents two peaks. The low temperature peak increases with the system size L and coincides with the temperature at which the order parameter (6) decays. Thus, it is associated with the stripe-tetragonal phase transition [7]. The temperature of the corresponding maximum of the specific heat appears to be almost independent of the system size, a finite size behavior usually observed in second order phase transitions. The second broader peak at higher temperature does not depend on the system size and is associated with the continuous decay of the tetragonal into the paramagnetic phase. This second peak becomes more pronounced as δ increases [7].

The existence of the tetragonal phase was first predicted by Abanov and coauthors [17] in a continuous approximation for ultrathin magnetic films, and it was only recently verified experimentally in fcc Fe on Cu(100) films [18, 19]. The work of Abanov *et al.* also predicted that the stripe-tetragonal transition should be either first order or the two phases might be separated a third phase characterized by rotational domain wall defects, that they called an *Ising nematic phase* [17]. Neither the Monte Carlo results of Booth *et al.*, nor the experimental results have shown any evidence of this phase. However, the results of Booth *et al.* appear to be consistent with a *second* rather than a first order transition, as expected from Abanov *et al.* results. Nevertheless, Booth *et al.* pointed out that the possibility of a weak first order transition cannot be excluded from their Monte Carlo calculations. Indeed, extensive Monte Carlo calculations in other region of the parameters space showed that this is the case [9]. Information about the order of the

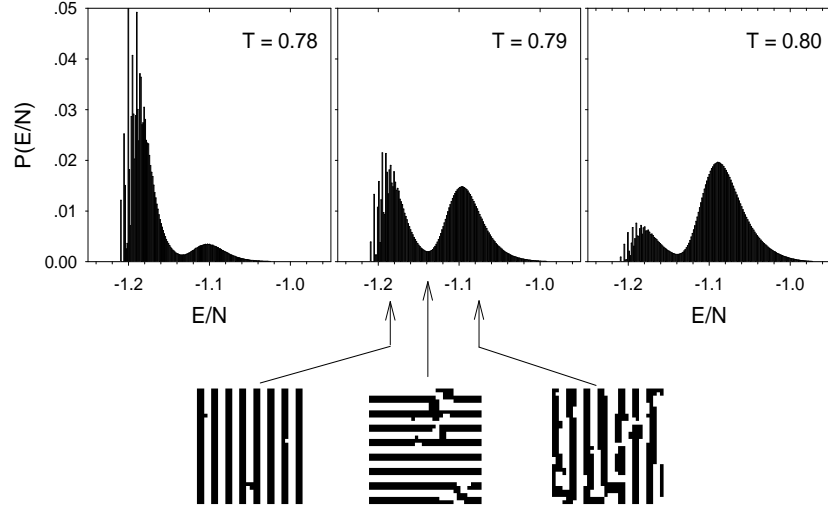


FIG. 7: Energy per spin histograms for $\delta = 2$, $L = 32$ and different temperatures around the pseudo-critical one $T_c^{(1)}(32) \approx 0.79$. Some typical equilibrium configurations for the indicated energies are also shown.

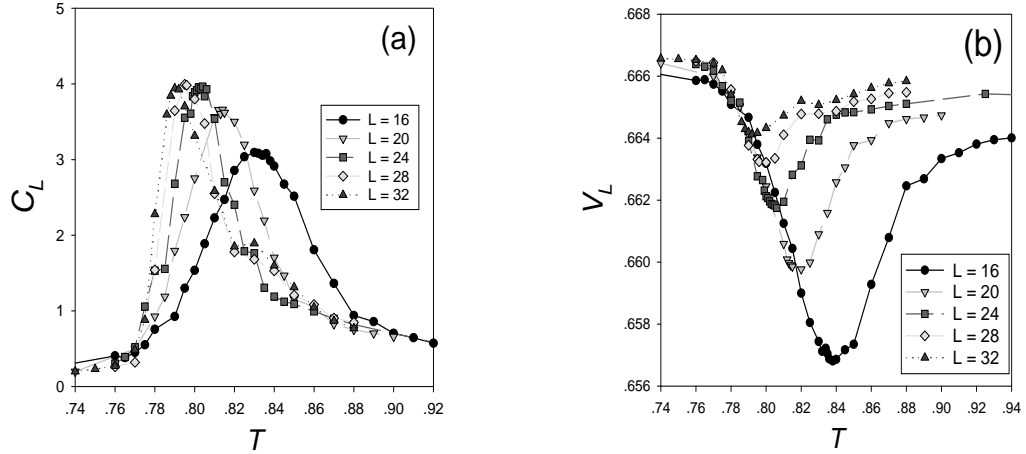


FIG. 8: Monte Carlo calculations for $\delta = 2$ and different system sizes. (a) Specific heat; (b) Binder cumulant.

transition can be obtained by analyzing the energy per spin histograms obtained during a single, large run of a Monte Carlo simulation for different temperatures, as in the example shown in Fig.7 for $\delta = 2$. The double peak structure of the energy distribution is characteristic of a first order phase transition. The typical configurations associated with each peak (i.e., with energies around the maxima) depicted in Fig.7 show that the low and high energy peaks are associated with the striped ($h = 2$) and the tetragonal phases respectively. The typical configurations associated with the minimum of the distribution correspond to a coexistence of both phases. Further evidence of the first order nature of the transition can be obtained from finite size scaling properties of the specific heat (2) and the Binder fourth order cumulant [20]:

$$V_L \equiv 1 - \frac{\langle H^4 \rangle}{3 \langle H^2 \rangle^2} \quad (7)$$

The last quantity presents a monotonous behavior at the critical temperature if the transition is continuous [20]. If the transition is first order, $V \rightarrow 2/3$ both for $T \ll T_c$ and for $T \gg T_c$ (when $L \rightarrow \infty$) and presents a minimum around

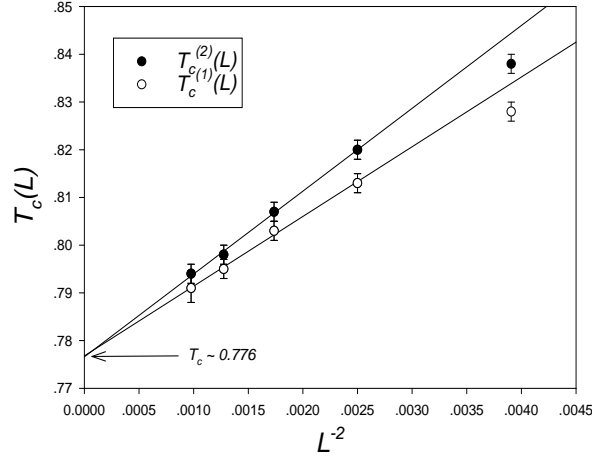


FIG. 9: Pseudo critical temperatures $T_c^{(1)}$ (maximum of the specific heat) and $T_c^{(2)}$ (minimum of the Binder cumulant) vs. L^{-2} for $\delta = 2$.

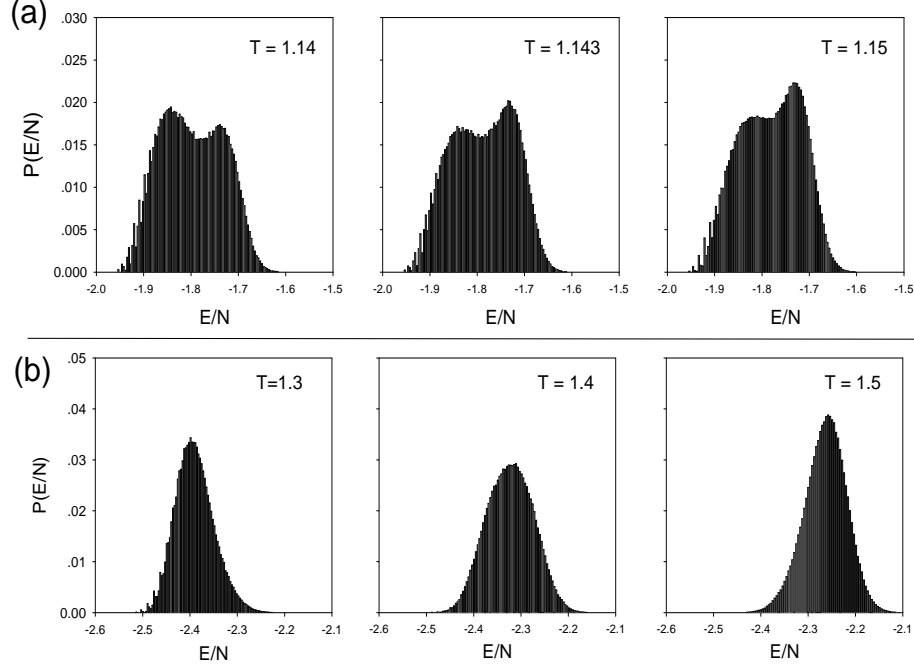


FIG. 10: Energy per spin histograms for $L = 24$ and different temperatures around the pseudo-critical ones $T_c^{(1)}(L)$. (a) $\delta = 2.6$; (b) $\delta = 3$.

some pseudo-critical temperature $T_c^{(2)}(L)$ [20]. In a first order temperature-driven phase transition the specific heat presents a maximum at a different pseudo-critical temperature $T_c^{(1)}(L) < T_c^{(2)}(L)$. In Fig.8 we see a Monte Carlo calculation of $C_L(T)$ and $V_L(T)$ for $\delta = 2$ and different system sizes [9]. The strong dependency of $T_c^{(1)}(L)$ and $T_c^{(2)}(L)$ on L are characteristic of first order phase transitions. Moreover, the plot of those quantities as a function of L^{-2} shown in Fig.9 verify the expected finite size scaling behavior in a first-order temperature driven phase transition [21]: $T_c^{(1)}(L) \sim T_c + AL^{-2}$ and $T_c^{(2)}(L) \sim T_c + BL^{-2}$ with $B > A$, T_c being the transition temperature of the infinite system.

Notice that the internal energies of both phases (roughly corresponding to the energies of the maxima of the histogram) near the transition temperature are located very close to each other. This property is also reflected in the rather shallow shape of Binder cumulant around $T_c^{(2)}$ (see Fig.8b) and evidences the weak nature of the transition.

This effects become more pronounced as δ increases. Moreover, for values of $\delta > 2.6$ the double peak structure (together with the minimum of the Binder cumulant) seems to disappear, or at least become undetectable for small system sizes, as can be seen in Fig.10. This fact explains the seemingly continuous nature of the transition observed by Booth *et al.*, whose calculations were performed for $\delta \geq 3$ [7]. However, analytic calculations on a related continuous model suggest that it belongs to a large family of systems, or universality class, in which a first transition for *any* value of δ is expected on quite general grounds [9]. So, the question of the order of the transition for large values of δ still remains open.

III. DYNAMICAL PROPERTIES

The dynamics of the two-dimensional Hamiltonian (1) at low enough temperatures is characterized, as occurs with any magnetic system that presents long-range order, by the formation and growth of small regions of ordered spins called *domains*. But unlike other magnetic models without disorder in the Hamiltonian, in this particular case the competition between the short range ferromagnetic interactions (that induces the system to order) and the dipolar antiferromagnetic interactions (that frustrates it and tends to increase the degeneracy of the ground state) gives place to an unusual slowing down of the dynamics. And this peculiar behavior somehow resembles that observed in systems with imposed disorder (i.e., with randomness in the Hamiltonian), such as, for instance, Edwards–Anderson spin glasses and random field Ising models. This is not a minor point, at least from a statistical mechanics point of view, mainly because there has been a considerable effort during the last years in trying to find a lattice model able to catch many of the dynamical and thermodynamical properties of structural glasses, which also present a notorious slowing down of the dynamics. And unlike spin glasses, it is nowadays vastly accepted in the community that an adequate model for structural glasses can not include disorder in the Hamiltonian. On the contrary, all the complexity of their dynamical behavior should be explained only in terms of the competition between the short range repulsion and long range attraction character of a some *Lennard–Jones*–like molecular interactions. Although a complete discussion about those attributes that can make a lattice system an acceptable model for structural glass is out of the scope of this article, we will revisit this point below, in order to show some recent evidence that permit us to suspect that Hamiltonian (1) could be considered a good candidate for modelling a bidimensional structural glass system.

Let us come back to the *thin-film* interpretation of model (1), which in fact is shared by almost all the authors who have contributed to its study during the last years. In 1996, Sampaio, Albuquerque and de Menezes performed a detailed study of the relaxation dynamics and hysteresis effects of the model [23]. In particular, starting from a fully magnetized configuration, they numerically analyzed the way the magnetization relaxes when the magnetic field is suddenly switched off. Inside the striped phases, where the equilibrium magnetization is obviously zero, they surprisingly found two different dynamical regimes, depending on the value of δ . For $\delta \geq \delta_c \equiv 1.35$ the initially fully magnetized state quickly relaxes to equilibrium, following the expected exponential law characterized by a strong dependence on both δ and temperature T . On the other hand, when $\delta < \delta_c = 1.35$ the relaxation presents a power law behavior with an exponent that does not depend on δ . This last behavior, usually found in systems with imposed disorder, motivated new investigations about the nature of the dynamical behavior of the model.

Hence, in the next three subsections we will present and discuss those results that have been found during the last years concerning the out of equilibrium dynamics of Hamiltonian (1).

A. Aging

Aging is one of the most striking features in the off-equilibrium dynamics of many complex systems. It refers to the presence of strong memory effects spanning time lengths that in some cases exceed any available observational time. Unfortunately, the large body of experimental evidence accumulated on the aging phenomena has not yet lead to a substantial understanding of the microscopic principles that can give origin to this complex phenomenology. Aging phenomena are so relevant mainly because some kind of *universality* appears in its description which makes it possible to categorize different systems as members of different classes. The main feature of aging is the conjunction of extremely slow dynamics together with non stationary relaxation functions. In fact, a system that ages loses the time translation invariance. That means that all statistical quantities that depend on two times, do not depend only on their difference, as occurs in an equilibrated state.

Although aging has been seen in a wide variety of contexts and systems [27] (some of them, actually very simple ones [30]) it is perhaps in the realm of magnetic and structural glasses dynamics where a systematic study of these phenomena has been carried out (see [27] and references therein).

In real materials, aging can be observed, for instance, in a Thermo–Remanent Magnetization (TRM) relaxation experiment: the system is abruptly cooled under a magnetic field \vec{B} that is switched on at $t = 0$, when the system is

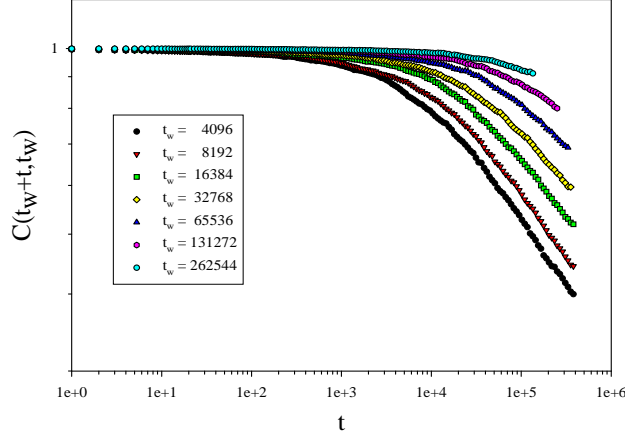


FIG. 11: Autocorrelation function $C(t_w + t, t_w)$ vs. t for $\delta = 2.0$, $T = 0.25$ and different waiting times t_w .

quenched at $T < T_c$, up to a time t_w when it is suddenly turned off. One then verifies that the magnetization M at time $\tau + t_w$ depends both on τ and t_w , with $\lim_{t_w \rightarrow \infty} M(t_w + \tau, t_w) \equiv M(|\tau|)$. One can also measure aging by looking at the two-time autocorrelation function $C(t, t')$. Although it is hard to measure autocorrelation functions in a real experiment, it is very simple to calculate it in a numerical experiment. For an Ising system like the one considered in this article, the autocorrelation is defined as:

$$C(t_w + \tau, t_w) = \frac{1}{N} \sum_{i=1}^N S_i(t_w + \tau) S_i(t_w) \quad (8)$$

In these numerical experiences it is not necessary to consider an external magnetic field. The system is simply quenched at time $t = 0$ from a very high temperature (usually infinite temperature) below the transition temperature and let to evolve during certain *waiting time* t_w , when the configuration $\{S_i(t_w)\}$ is stored. From then on the two time autocorrelation function (8) is calculated. If the system attains an equilibrium state, then $C(t_w + \tau, t_w) = C(\tau)$. But, if the system does not equilibrate in a reasonable time, then C will explicitly depend both on τ and t_w , indicating the presence of aging.

There are basically two scenarios within which aging can emerge. On one hand, aging appears as a consequence of weak ergodicity breaking [27] and it is related to the complex structure of the region of phase space that the system explores in time. This is the case, for instance, in the Sherrington-Kirkpatrick (SK) [29] model and other spin glass models in which the complexity of the energy function is associated to a certain degree of randomness and/or frustration in the Hamiltonian. On the other hand, the onset of aging in many systems derives from the presence of coarsening processes that give place to a drastic slowing down of the dynamics. In this case the scaling law of the two-time autocorrelation function is ruled by the following expression

$$C(t + t_w, t_w) \sim f(L(t)/L(t_w)), \quad (9)$$

where $L(t)$ is the mean linear size of the domains at time t [28].

In Fig. 11 we see a typical behavior of $C(t_w + t, t_w)$ inside the striped phase for $\delta = 2.0$, $T = 0.25$ and different values of t_w . Clearly we verify the presence of aging, identified by the strong dependence on both t and t_w . For a given t_w we observe that the system stays in a quasi-equilibrium state before $C(t_w + \tau, t_w)$ finally relaxes to zero. Furthermore, as the time the system spends in the ordered phase t_w increases, the time the system spends in the quasi-equilibrium state also increases (this phenomenon is the origin of the name *aging*).

An insight about the nature of the aging phenomena observed inside the striped phase can be obtained by analyzing the scaling properties of $C(t + t_w, t_w)$ in different regions of the phase diagram, which can tell us about the universality class of the dynamical regime. Indeed, there seems to be two different dynamical regimes [24], depending on the value of δ . When $\delta > \delta_c$ and $T = 0.25$, $C(t + t_w, t_w)$ displays the scaling form:

$$C(t + t_w, t_w) \propto f\left(\frac{t}{t_w}\right). \quad (10)$$

while for $\delta < \delta_c$ at the same temperature the results seems to be consistent with a logarithmic scaling law of the

form [24]:

$$C(t_w + t) \propto g\left(\frac{\ln(t)}{\ln(t_w)}\right). \quad (11)$$

Let us extract now some conclusion of these results. If the slowing down of the dynamics is ruled by the domain growth process, as expected in this kind of model without disorder, after a certain time t one can measure the average linear domain size $L(t)$. The time evolution of quantities like the autocorrelation function will then present a crossover from the dynamical regime characterized by length scales smaller than the domain size $L(t_w)$ to a regime at larger scales, dominated by domain growth through the movement of domain walls. In this scenario, scaling arguments lead to the following (and already mentioned) dependency of $C(t_w, t_w + t)$

$$C(t_w, t_w + t) \propto \Theta\left(\frac{L(t_w + t)}{L(t_w)}\right) \quad (12)$$

Hence, when $t \gg t_w$

$$C(t_w, t_w + t) \rightarrow \Theta\left(\frac{L(t)}{L(t_w)}\right) \quad (13)$$

is expected.

Summarizing, the results for $\delta > \delta_c$ are consistent with an algebraic growth of the linear domain size of the form $L(t) \propto t^\psi$. But what emerges as a much curious result is the behavior observed for $\delta < \delta_c$, which appears to be consistent with a logarithmic time dependence of the average domain size $L(t) \propto (\ln(t))^\psi$ predicted by an activated dynamic scenario proposed by Fisher and Huse [31] in the context of spin glasses, in which both disorder and frustration generate active droplets excitations with a broad energy distribution.

Another consequence of the loss of the time invariant translation of a system that ages during its relaxation, is the violation of the Fluctuation Dissipation Theorem (FDT). Let us suppose that an inhomogeneous external magnetic field $h_i(t)$ is switched on at time t_w ; the conjugate response function at time $t_w + t$ can be defined as

$$R(t_w + t, t_w) = \frac{1}{N} \sum_i \frac{\partial \langle S_i(t_w + t) \rangle}{\partial h_i(t_w)} \quad (14)$$

Let us now assume that the system has attained true thermodynamical equilibrium. Then, time translational invariance holds and both the autocorrelation and the response functions depend only on the time difference t and the FDT gives us a precise relationship between $R(t)$ and $C(t)$:

$$R(t) = \frac{1}{T} \frac{\partial C(t)}{\partial t}. \quad (15)$$

For a system that ages, as the one studied in this paper, one can identify two different regimes, as we have already seen: for small values of t ($t/t_w \ll 1$) the system is in a quasi-equilibrium state, at least for large t_w , and all the equilibrium properties hold. But in the aging regime, when $t \gg t_w$, both the time translation invariance and the Fluctuation Dissipation Theorem do not hold. In other words, $C(t_w + t, t_w)$ and $R(t_w + t, t_w)$ depend explicitly on t and t_w . In particular, for a great variety of disordered models and also during some coarsening processes, in this last regime a generalized version of the FDT holds, which asserts that

$$R(t_w + t, t_w) = \frac{X(t + t_w, t_w)}{T} \frac{\partial C(t + t_w, t_w)}{\partial t_w} \quad (16)$$

with $X(t + t_w, t_w) \neq 1$. Moreover, for large enough values of t_w , $X(t + t_w, t_w)$ becomes a function of time only though $C(t_w + t, t_w) = X(C(t + t_w, t_w))$. The function $T/X(C)$ can be now interpreted as a non-equilibrium *generalized temperature*. This kind of analysis has also been applied in [25] to model (1). Surprisingly, it was found that the system behaves in the same way, irrespectively of the value of δ . Actually it was observed that, as $t_w \rightarrow \infty$, the generalized temperature tends to zero, which is a clear signature of a coarsening process.

B. Coarsening

As we have already seen, when a magnetic system is suddenly quenched from a very high temperature (above the critical temperature T_c) into the ordered phase, small clusters of ordered spins form which are usually called

domains. Immediately after the cooling the system finds itself in a disordered state induced by the abrupt quench, but accordingly to the thermodynamical laws, it would evolve into an ordered state. Under these circumstances the small domains of ordered states start growing, in a process that is usually called *coarsening*. If we could take a snapshot of the system a few seconds after the quench, we would identify a patchwork of small domains, ordered in so many different forms as different ground states the system admits. But, since there is a interfacial free energy cost associated with the surface of the boundary between domains, as the domains grow they compete with each other in order to impose their own order. As a consequence of this competition, the patchwork of domains evolves in time, trying to decrease the free-energy of the whole system by decreasing the area of the interface region between domains.

Coarsening is an ubiquitous phenomenon in nature that largely exceeds the realm of magnetism [32]. Even more, coarsening plays a fundamental role in many industrial processes, as for instance in molten iron. When the molten iron is suddenly quenched below the melting temperature, the originally dissolved fraction of carbon present in the system precipitates out. If the quench is fast enough, the carbon can not float to the top but stays dispersed through the iron forming small particles, and many of the relevant properties of cast iron depends specifically on the size and form of the carbon small clusters. Hence, controlling the quality of the iron requires a precise knowledge of the coarsening process of carbon particles. Other examples of coarsening in physical systems appear in foams, the ordering of binary alloy following a quench from above to below its order-disorder transition temperature and the phase separation of a binary fluid following the quenching from the one-phase to the two-phase region of its phase diagram.

The simplest way to characterize the coarsening process is by measuring the time evolution of the *characteristic domain linear size* $L(t)$. This procedure, which is hard to carry out in an experiment, can be easily implemented in numerical simulations of Ising models like the ones presented in this article. Coarsening has been vastly studied during the last decades, both experimentally and theoretically, but there are still many open questions, especially concerning the role of frustration in the time evolution of $L(t)$. The domain growth scenario in the ferromagnetic phase of the Ising model is very much alike the critical dynamics observed in the neighborhood of a critical point. The competition among the different domains trying to impose their order to the whole system (as discussed above) yields to a power law behavior of the average linear size $L(t)$

$$L(t) \propto t^n \quad (17)$$

Note that this critical-like slowing down of the dynamics occurs even far away from the critical point. Since the domain linear size $L(t)$ will eventually reach macroscopic length scales one can expect that the coarsening exponent n will be independent of many of the microscopic details. In other words, there should be only a few dynamical *universality classes*, as in fact occurs in the study of critical phenomena. Two of these universality classes are already well understood. The first class corresponds to the case of a microscopic dynamics that preserve the order parameter of the system, and they are characterized by an exponent $n = 1/3$. They are usually called *Lifshitz-Slyozov* [33] growth processes, and a typical realization is the spinodal decomposition. The second class is associated to those microscopic dynamics for which the order parameter is not conserved, and they are characterized by an exponent $n = 1/2$. As we indicated in IIB, our simulations were all performed using a heat bath or Metropolis Monte Carlo dynamics which correspond to this second universality class, usually called *Lifshitz-Allen-Cahn* or *Curvature-driven* growth [34, 35]. A typical physical example is given by the process of grain growing in metals.

But, there is also a third universality class observed in systems with imposed disorder, i.e., in systems whose Hamiltonian includes, besides the dynamical variables, a set of random variables necessary to describe the structural randomness of the system. In these cases the coarsening process departs from the usual power law of Eq. (17) and is characterized by a logarithmic growth rule of the form:

$$L(t) \sim \ln(t) \quad (18)$$

Spin glasses, random field models and models with random quenched impurities, are all examples of this third universality class. During many years it was not clear whether this behavior was restricted to systems with imposed disorder. Nowadays it is believed that the departure from the power law dynamics is related to the existence of free energy barriers that the coarsening system has to overcome which grow linearly with $L(t)$ [26]. In fact, there are also a few examples of systems with logarithmic coarsening that do not present randomness in the Hamiltonian, as for instance the three dimensional Ising model with nearest-neighbors ferromagnetic interactions and next-nearest-neighbors antiferromagnetic interactions, whose dynamics has been described by Shore, Holzter and Sethna in [26] (from now on we will refer to it as the Shore model, even when it has already been analyzed by other authors[38]). What seems to be the fundamental ingredient for the appearance of logarithmic coarsening is existence of a certain degree of frustration in the microscopic interactions.

When coarsening is analyzed at zero temperature, it is relatively easy to determine numerically the domain growth law. But when the system is analyzed at a non zero temperature new challenges emerge. In particular, it is very hard to distinguish real domain structures from occasional small clusters generated by thermal fluctuations. One way to

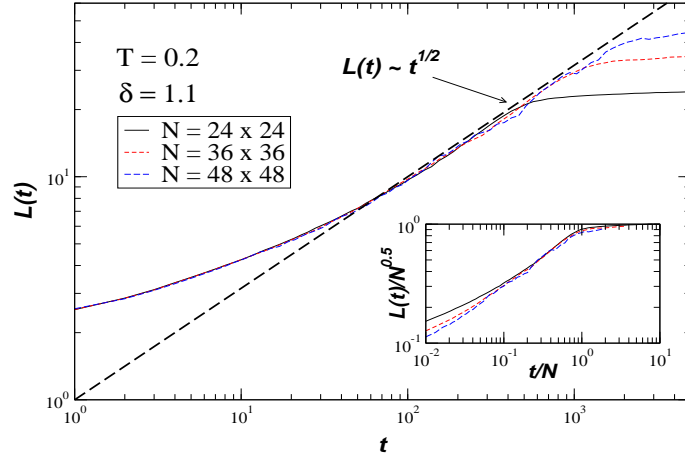


FIG. 12: Characteristic linear domain size $L(t)$ as a function of t for $\delta = 1.1$, $T = 0.2$ and three different system sizes. The dashed line indicates the curve $L(t) \sim t^{1/2}$.

overcome this difficulty is to use a technique based on the spreading of damage method proposed by Derrida [36] and later on improved by Hinrichsen and Antoni [37]. The method compares, as time goes on, the state of a suddenly quenched system with replicas of the same system initialized in the corresponding ground states. In particular, one needs to take into account the time evolution of so many replicas as possible ground states the system admits. Remember that in our case, the system has, depending on the value of δ , $4h$ possible ground states, which makes it very difficult to apply this technique for large values of δ . Both the quenched system and all its replicas evolve under the same thermal noise or, in other words, using the same random sequence in the updating process. All those spin flips that occur simultaneously in the quenched replica and in one of the ground state systems are considered thermal fluctuations, and they are not taken into account in the calculus of the domain areas.

We will summarize now the results of the coarsening dynamics of Hamiltonian (1), which are presented in detail in [16]. We focus our analysis in the particular case in which the system is quenched into the $h=1$ phase for values of $0.8 \leq \delta \leq \delta_{1,2}$ (see Fig. 3). To characterize the domain growth, the domain areas $A(t)$, defined as the number of spins inside each ordered cluster are first calculated. Then, the characteristic linear domain size is calculated as $L(t) = \sqrt{A(t)}$. Note that in this particular case, the spreading of damage method required a simultaneous comparison among five different replicas of the system (one for the quenched replica plus four for each possible ground state).

In Fig. 12 we present the behavior of the characteristic linear domain size $L(t)$ when $\delta = 1.2$ and $T = 0.2$, for three different system sizes $N = L \times L$ with $L = 24, 36$ and 48 . Remember that in this point of the phase space there are no metastable states (see Fig. 3). We observe that after a very short transient the system enters into the expected coarsening regime $L(t) \sim t^{1/2}$, as corresponds for a dynamics that does not preserve the order parameter. For large times, we see that $L(t)$ saturates in a value that coincides with $N^{1/2}$, indicating that the domain sizes have reached the size of the system. However, in IID we have seen that inside the ordered phase one can identify two different situations. In particular, for $\delta = 1$ we known that at low enough temperatures (actually for $T < 0.4$) there are also metastable states corresponding to stripes of width $h = 2$.

In order to determine the effect of these metastable states in the domain dynamics of the model, let us consider what happens when the final temperature of the quenching is lowered. In Fig. 13 we show the time evolution of $L(t)$ when $\delta = 1$ and $N = 24 \times 24$ for eight different temperatures, ranging from $T = 0.2$ to $T = 0.05$. What emerges from this analysis is the appearance of a new dynamical regime associated with the existence of metastability. When $0.1 < T < 0.2$ the system displays always the same behavior described in Fig. 12. But, for $T \leq 0.1$ a regime of slow growth develops at intermediate time scales before the system crosses over to the $t^{1/2}$ coarsening regime. As we lower the temperature further, this intermediate regime extends to larger time scales; nevertheless, all the curves eventually cross over to the $n = 1/2$ regime. Note that for short times there seems to be a change in the concavity of the curves $L(t)$ when the final quenching temperature crosses the value $T = 0.1$, which coincides, for $\delta = 1.1$ with the spinodal boundary of the metastable phase of width $h = 2$ inside the equilibrium phase of width $h = 1$.

To characterize further the behavior of the linear domain size $L(t)$ let us consider the crossover time τ , given by the intersection of the power law branch of the curve and the horizontal saturation branch. In Fig. 14 we show a plot of τ as a function of T . While for temperatures greater than $T = 0.1$ the crossover time presents a linear dependency with $1/T$, in the region of metastability $T \leq 0.1$ we observe an exponential increasing of τ as $1/T$ increases, as can

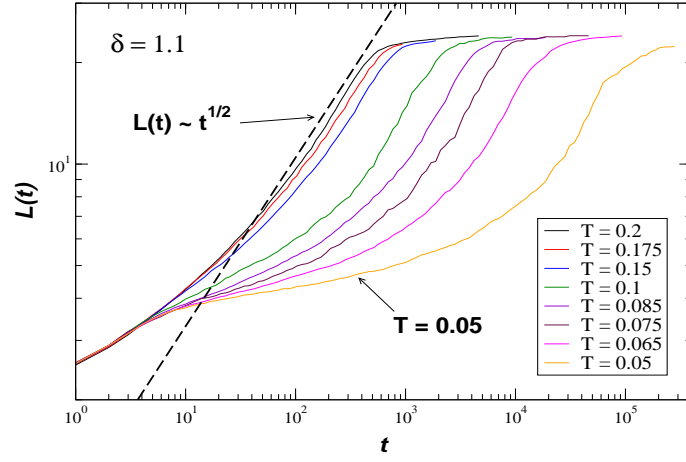


FIG. 13: Characteristic linear domain size $L(t)$ as a function of t for $\delta = 1.1$ and $N = 24 \times 24$ and eight different temperatures indicated in the figure.

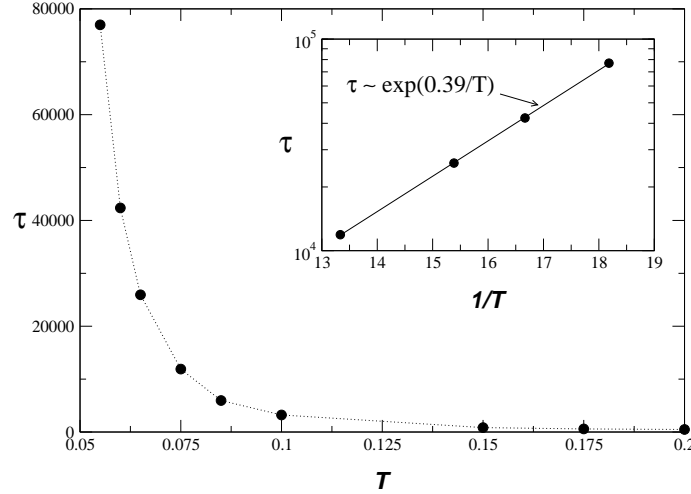


FIG. 14: Crossover time τ vs. T for $\delta = 1.1$ and $N = 24 \times 24$. On the inset, an Arrhenius plot of τ vs. $1/T$ for the four lower temperatures showed in Fig. 14. The straight line in the inset indicates the best fitting.

be deduced from the Arrhenius plot presented in the inset of Fig. 14. The straight line denotes the best linear fit, given by

$$\tau = 62.5 \exp(0.39/T) \quad (19)$$

In Fig. 15 we present a temporal sequence of snapshots of a system of $L = 48$ spins and $\delta = 1.1$ at $T = 0.2$, where the system does not present the slow intermediate regime. The pictures appear in pairs. The left pictures correspond to configurations of the system at different times, where black points indicate spins up and white points spins down. In the right pictures we can visualize the corresponding domain walls obtained with the method of Hinrichen and Antoni [37], previously described. Here the black points represent spins inside a domain while the white points indicate spins that belong to the domain wall. Starting from the left top the snapshots correspond to time steps $t = 1, 10, 20, 30, 40, 50, 100, 200, 300$ and 400 . After a few time steps, certain degree of local order is achieved, and we can identify small clusters of striped structures. As the system evolves small domains appears, which can be identified in the right pictures as black areas (see $t = 30$ and $t = 40$). These small domains start to grow and the coarsening process can be easily observed (compare $t = 50$ and $t = 100$). Note that some domain walls are still very thick, and seem to persist longer times. The domain walls tend to align in a diagonal direction. We can see that once a thick domain

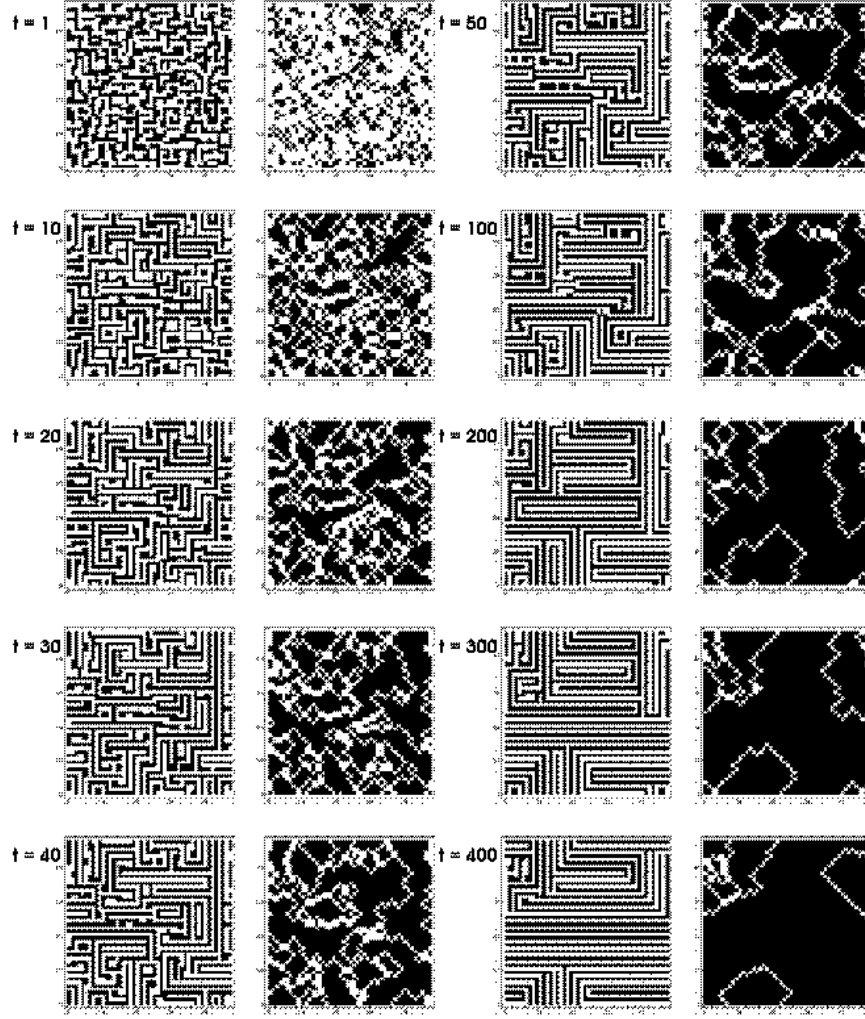


FIG. 15: Snapshots of the coarsening process when a system with $\delta = 1.1$ and $N = 48 \times 48$ spins was quenched to $T=0.2$

wall disappears the domain boundary around it quickly moves. In other words, thick walls seem to pin the motion of thin walls.

Finally, in Fig. 16 we present a new sequence, but now obtained by suddenly quenching a system with $\delta = 1.1$ and $N = 48 \times 48$ into the metastability region, at $T = 0.05$. Note that the first five snapshots are similar to the first five snapshots of the coarsening process at $T = 0.2$. Small domains appear of stripes of width $h = 2$ (compare the time scales of this figure and the former). In the high temperature coarsening this small blocks do not seem to play a fundamental role in the growth of the domains. However, in the snapshots of the low temperature coarsening it is clear that this blocks slow the domain growth. Even more, these blocks seem to pin the domain walls and slow the dynamics. In other words, the crossover from the slow logarithmic regime to the $t^{1/2}$ regime will be characterized by the time needed to depin this blocks and free the domain walls. These dynamical behaviors present a strong resemblance with the ones observed in the two dimensional Shore model [26]. The presence of NNN antiferromagnetic bonds in this model introduce free-energy barriers to domain coarsening that are independent of the domain size L [26]. Such barriers in this model are a consequence of a corner rounding process which generates structures that block the coarsening dynamics [26]. Hence, the system is stuck and coarsens little on time scales $t \ll \tau_B(T) = \exp(F_B/T)$ (F_B being the height of the barrier), while on time scales $t \gg \tau_B(T)$ the free-energy barrier can be crossed and the $t^{1/2}$ behavior emerges. In fact, the time to completely shrink squares of h_2 phase immersed in an h_1 phase coincides with the divergence observed in the crossover time from the slow growth to the $t^{1/2}$ regime [16]. These results are consistent with the presence of free-energy barriers independent of the domain size L , associated with blocking clusters of the metastable phase, which generates a crossover in the coarsening behavior as we cross the spinodal line. Since

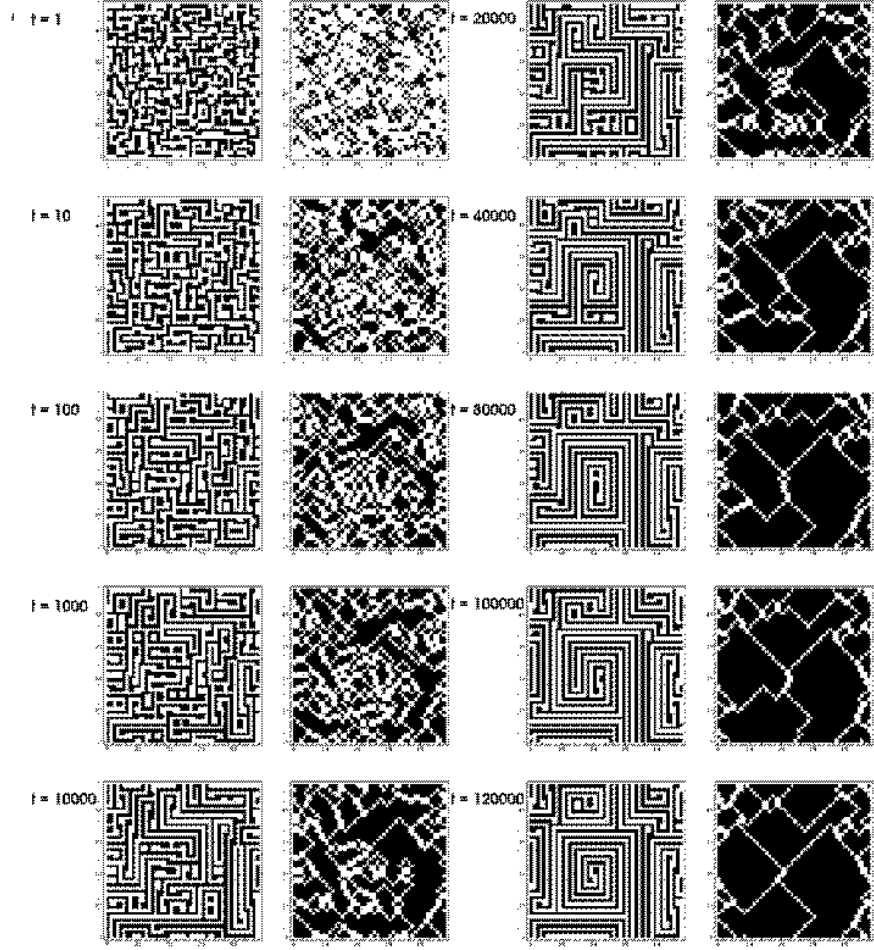


FIG. 16: Snapshots of the coarsening process when a system with $\delta = 1.1$ and $N = 48 \times 48$ spins was quenched to $T=0.05$

the cross over time diverges as the temperature is lowered, the very slow behavior at intermediate times may be indistinguishable from a logarithmic law.

C. Slow cooling

As we have already seen, at very low temperatures where metastability effects appear, the system displays an intermediate slow regime. Nevertheless, after certain period of time that diverges as $T \rightarrow 0$, it finally enters into the expected algebraic regime $L(t) \propto t^{1/2}$. In this subsection we present another interesting way of analyzing the out of equilibrium dynamics of the model. Starting from a thermalized state above the transition temperature, we measure the average domain linear size $L(t)$ when the temperature is slowly lowered below the transition temperature.

To simulate the slow cooling, the procedure is as follows [16]: the system is initially thermalized at certain temperature T_0 above the transition between the ordered and the disordered phases and then we lower the temperature during the Monte Carlo simulation at a constant rate

$$T = T_0 - rt, \quad (20)$$

where r denotes the constant cooling rate of the experiment. Once the system has reached the state with $T = 0$ one calculates the average linear domain size L_0 at the end of the cooling process. Since the dynamics gets trapped by the coarsening process, the system will never reach the ground state for any non-zero values of r . Furthermore, L_0 strongly depends on the cooling rate r and on the coarsening universality class of the system [40]. For a glassy system, characterized by the logarithmic domain growth law (18) the relationship between L_0 and r is also logarithmic:

$$L_0 \sim -\ln(r) \quad (21)$$

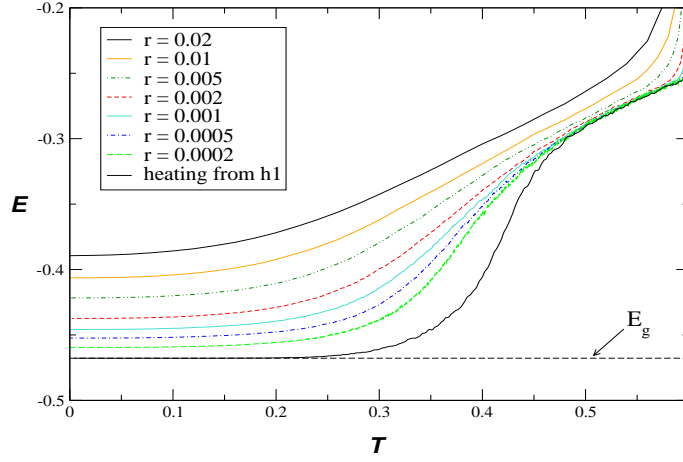


FIG. 17: Internal energy E as a function of temperature T for seven different cooling rates, (from top to bottom) $r = 0.02$, 0.01 , 0.005 , 0.002 , 0.001 , 0.0005 and 0.0002 , for $N = 64 \times 64$ and $\delta = 1$. The lowest curve corresponds to a heating process from the ordered states (striped state with $h = 1$). The dashed line indicates the ground state energy $E_g = -0.467758$.

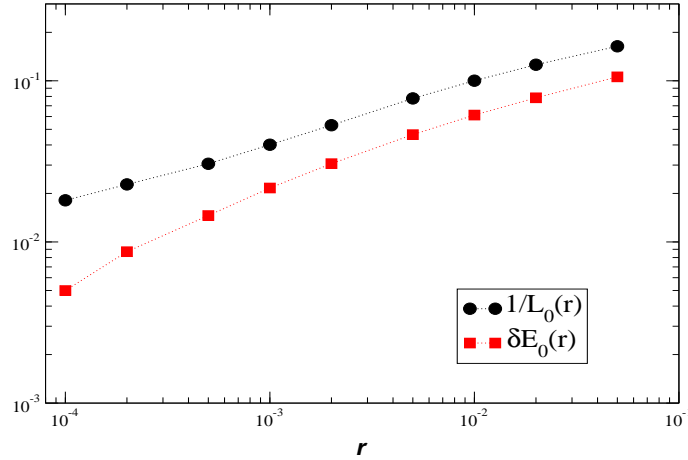


FIG. 18: Excess energy δE and $1/L_0(r)$ as a function of the cooling rate r for $\delta = 1.0$.

while for a system that follows an algebraic coarsening law one finds a much faster growth of the form:

$$L_0 \sim r^n, \quad (22)$$

with $n = 1/2$ or $n = 1/3$ depending on the particular dynamics.

Along the simulations one can also monitor the energy excess $\delta E(r) = E_0(r) - E_g$ where $E_0(r)$ is the final value of the energy when the system is cooled at rate r and E_g is the energy of the ground state. In Fig. 17 we show the temperature dependence of the internal energy E for seven different cooling rates $r = 0.02$, 0.01 , 0.005 , 0.002 , 0.001 , 0.0005 and 0.0002 , for a system of size $N = 64 \times 64$ and for $\delta = 1.0$ (inside the striped phase of width $h = 1$).

In Fig. 18 we plot both $1/L_0(r)$ and δE_0 as a function of the cooling rate r . The quantity $L_0(r)$ was calculated by using the method proposed by Cirilo *et al.* in [39]. The best fits gave for both quantities a power law behavior

$$\delta E(r) \propto r^{0.35} \quad \text{and} \quad L_0(r) = 1.9^{-0.37} \quad (23)$$

which can not be interpreted neither as a logarithmic nor as the $n = 1/2$ algebraic law. But this behavior can be easily understood: when the system is slowly cooled from the disordered phase into the metastability region, it must pass through the fast dynamics temperature range, which allows the system to form certain local order at a fast rate, before it enters into the slow intermediate regime.

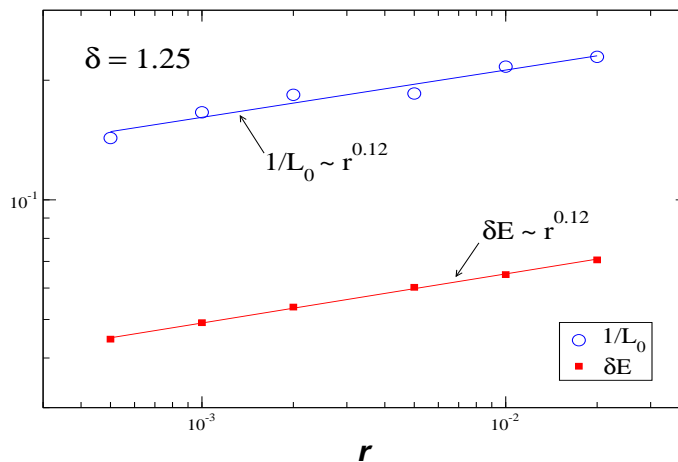


FIG. 19: Excess energy δE and $1/L_0(r)$ as a function of the cooling rate r for $\delta = 1.25$.

To verify the former scheme let us consider the slow cooling of a system with $\delta = 1.25$, which is near the border between the $h = 1$ and $h = 2$ striped phases. We chose this value because in this particular case the system passes directly from the disordered phase into the metastability region without entering in a fast dynamics regime (see Fig. 3). In Fig. 19 we plot again both $1/L_0$ and δE vs. r for $\delta = 1.25$. The behavior of L_0 can be well fitted by a power law with a small exponent

$$L_0(r) \propto r^{-0.12}. \quad (24)$$

which is very hard to distinguish from a logarithmic law.

In order to understand in more details which is the mechanism responsible for this drastic slowing down, let us take a direct look into the configurations. In Fig. 20 we see four typical realizations of the spin configurations for the same system of $N = 64 \times 64$ spins with $\delta = 1$ and $\delta = 1.25$, respectively. The snapshots presented were obtained at $T = 0.2$ and $T = 0.1$. What we observe is that in the region of metastability ($\delta = 1.25$), domains of $h = 2$ structures develop which prevent the system to reach a larger order, being responsible of slowing down. On the other hand, we see that in the $\delta = 1.0$ case, these structures rapidly disappear, during the fast relaxation regime at intermediate temperature.

Concluding, we can see that the slow cooling experiments confirm that the metastability is the responsible of the slow relaxation dynamics observed in this two-dimensional model.

IV. DISCUSSION AND FURTHER DIRECTIONS

In this work we have presented a rather detailed description of the present state of the art concerning the macroscopic properties of the two dimensional Ising model with competition between nearest-neighbors interactions and long-range antiferromagnetic interactions in a square lattice. Our analysis focused on the nature of the different thermodynamical transitions for low values of δ and on the out of equilibrium dynamics in the low temperature phases of the model.

One of the most interesting thermodynamical properties is the weak first order nature of the order-disorder phase transition for some range of values of δ , predicted by extensive Monte Carlo numerical simulations. This result appears to answer the apparent contradiction between the prediction of Abanov [17] and Booth *et al.* results [7]. The challenge persist to determine experimentally the nature of this transition in ultrathin magnetic films [18]. A question that remains open refers to the order of the phase transition for large values of δ . While a continuous approximation predicts that the transition is first order for any value of δ on very general grounds [9], the Monte Carlo results appears to be consistent with a change in the order of the transition at some finite value of δ , above which the transition becomes continuous. Anyway, if the transition for large values of δ is so weak that it becomes indistinguishable from a continuous one, the difference could be irrelevant from the experimental point of view.

The existence of a first order transition of this type is also interesting for other reason. This behavior strongly resembles that observed in the three dimensional Coulomb frustrated ferromagnet [22, 41]. Hence, it opens the possibility to observe in a two dimensional model dynamical phenomena similar to that seen in fragile glassforming liquids [42]. Works along this line are in progress.

Another interesting point about the thermodynamics of this model is related to the existence of metastable striped states at low temperature for large values of δ , which generate complex dynamical behaviors. As we have seen, the

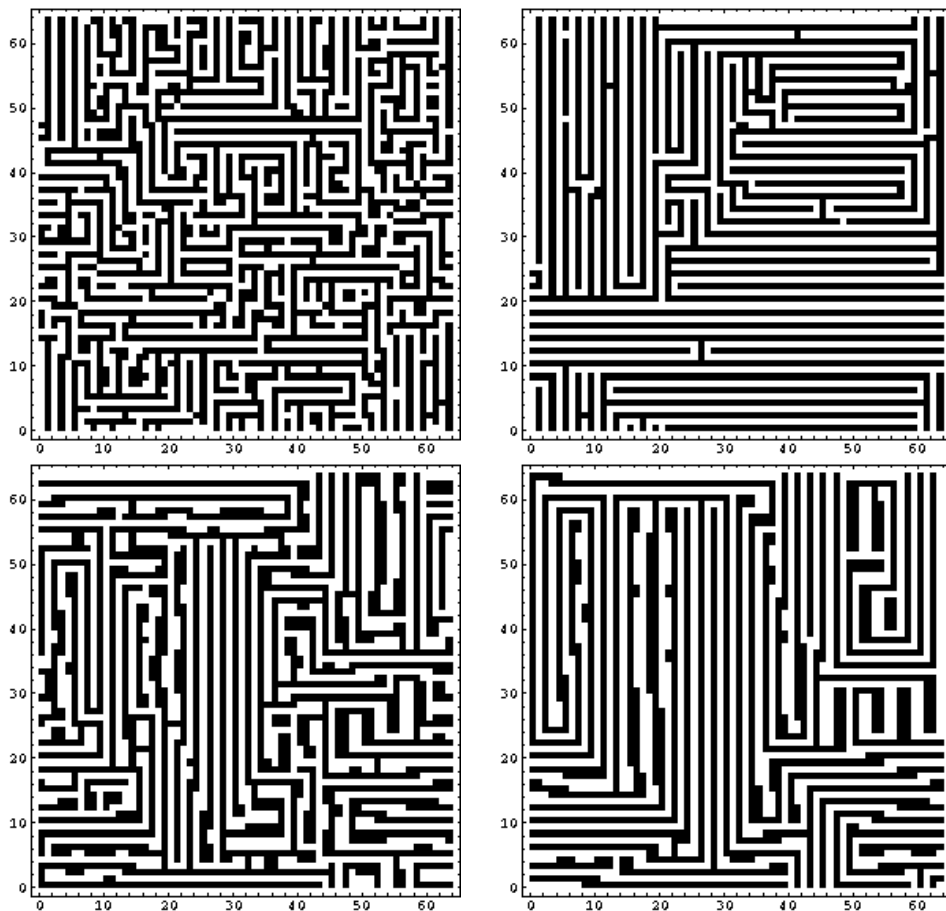


FIG. 20: Snapshot of a 64×64 cooled at a constant rate $r = 0.0001$. Upper figures: $\delta = 1.0$; lower figures $\delta = 1.25$. The left figures were obtained at $T = 0.2$ and the right ones at $T = 0.1$.

existence of metastable states at low temperatures reveals the true nature of the different dynamical regimes observed inside the striped phases. Some early works seemed to show contradictory evidence on the dynamical behavior of the system. On one side [24], there was evidence that for small values of δ the system presents a behavior similar to that observed in glassy systems (logarithmic growth of the linear domain size). On the other side, in [25] the authors found a behavior proper of a simple coarsening process (algebraic domain growth) in the same region. We have shown how different types of dynamical analysis allows one to interpret these apparently contradictory results, showing that the differences observed can be actually ascribed to the existence, at low temperatures, of a metastability region where metastable stripe states of different width coexist. The analysis of the striped domains growth shows that these metastable states trap the dynamics of the system during certain transient that diverges as $T \rightarrow 0$. When the system is quenched to the metastable region, small domains of the metastable phase pin the domain walls of the stable phase; such metastable domains generate free energy barriers whose height is independent of the domain size L , thus slowing the coarsening process for a finite (temperature-dependent) period of time. Measurements taken with observation time scales smaller than this characteristic periods display an apparently logarithmic behavior. Numerical experiments in which a slow cooling is performed from a thermalized state above the transition temperature give further support to this interpretation (see Fig.20).

The existence of multiple metastable ordered states at higher values of δ and very low temperatures opens other interesting perspectives. We expect that the domain walls of the stable phases should be pinned by clusters of the different coexisting metastable phases. Therefore, we expect a slow dynamics characterized by multiple characteristic time scales, associated with the different free energy barriers generated by each metastable phase.

We see that many of the open questions remarked above appear for large values of δ . Unfortunately, in this region finite size effects and the strong dynamical slowing down make numerical simulations prohibitive, since larger system sizes should be considered. The usage of more sophisticated non-Metropolis sampling methods, like a recent adaptation of Creutz cluster algorithm [10] or the multicanonical algorithm [43], may help, at least for studying equilibrium properties.

Finally, one important point of experimental importance [19] that remains to be answered concerns the role of defects in the high temperature order-disorder transition. Some advances along this line has been done recently in in the triangular lattice [10].

This work was partially supported by grants from Consejo Nacional de Investigaciones Científicas y Técnicas CON-ICET (Argentina), Agencia Córdoba Ciencia (Córdoba, Argentina) and Secretaría de Investigación Científica y Tecnológica de la Universidad Nacional de Córdoba (Argentina). P.M. Gleiser thanks Fundación Antorchas (Argentina) for financial support. We wish to thank H. Toloza, D. Stariolo and M. Montemurro for their fruitful contributions.

-
- [1] Pappas D.P., Kamper K.P. and Hopster H., 1990, Phys. Rev. Lett **64**, 3179.
 - [2] Allenspach R., Stampanoni M. and Bischof A., 1990, Phys. Rev. Lett. **65**, 3344.
 - [3] De'Bell, K., MacIsaac, A.B. and Whitehead, J.P., 2000, Rev. Mod. Phys. **72**, 225.
 - [4] MacIsaac, A.B., Whitehead, J.P., Robinson M.C. and De'Bell K., 1995. Phys. Rev. B **51**, 16033.
 - [5] It is worth noting that the definition of the Hamiltonian in [3, 4, 7] is slightly different from ours. While in those papers the dipolar term contains a sum over all pairs of spins, here we consider the sum over every pair of spins just once. This leads to the equivalence $\delta = J/2$, J being the exchange parameter in the above references. Since the dipolar parameter also fixes the energy units in our work, there is also a factor 1/2 between the critical temperatures obtained in those works and ours.
 - [6] Czech R. and Villain J., 1989, J. Phys.: Condens. Matter **1**, 619.
 - [7] Booth I., MacIsaac, A.B., Whitehead, J.P. and De'Bell K., 1995, Phys. Rev. Lett. **75**, 950.
 - [8] Gleiser P.M., Tamarit F.A. and Cannas S.A., 2002, Physica D **168–169**, 73.
 - [9] Cannas S.A., Stariolo D.A. and Tamarit F.A., *submitted*
 - [10] Stoycheva D.A. and Singer S.J., 2002, Phys. Rev. E **65**, 036706.
 - [11] Luijten E. and Blöte H.W.J., 1995, Int. J. Mod. Phys. C **6**, 359.
 - [12] Cannas S.A., Lapilli C.M. and Stariolo D.A., 2004, Int. J. Mod. Phys. C **15**, *in press*.
 - [13] Kretschmer R. and Binder K., 1979, Z. Phys. B **34**, 375.
 - [14] Allen M. P. and Tildesley D. J., 1990, *Computer Simulation of Liquids*, Clarendon Press, Oxford.
 - [15] Frenkel D. and Smit B., 1996, *Understanding Molecular Simulation*, Academic Press.
 - [16] Gleiser P.M., Tamarit F.A., Cannas S.A. and Montemurro M.A., Phys. Rev. B, *to appear* - eprint: cond-mat/0212617.
 - [17] Abanov A., Kalatsky V., Pokrovsky V. L. and Saslow W. M., 1995, Phys. Rev. B **51**, 1023.
 - [18] Vaterlaus A., Stamm C., Maier U., Pini M. G., Politi P. and Pescia D., 2000, Phys. Rev. Lett. **84**, 2247.
 - [19] Portmann O., Vaterlaus A. and Pescia D., 2003, Nature **422**, 701.
 - [20] Binder K. and Heermann D. W., 1992, *Monte Carlo Simulation in Statistical Physics*, 2nd Ed., Springer-Verlag.
 - [21] Lee J. and Kosterlitz J.M., 1991, Phys. Rev. B **43**, 3265.
 - [22] Grousson M., Tarjus G. and Viot P., 2001, Phys. Rev. E **64**, 036109.
 - [23] Sampaio L.C., de Albuquerque M.P. and F.S. de Menezes F.S., 1996, Phys. Rev. B **54**, 6465.
 - [24] Toloza J.H., Tamarit F.A. and Cannas S.A., 1998, Phys. Rev. B **58**, R8885.
 - [25] Stariolo D.A. and Cannas S.A., 1999, Phys. Rev. B **60**, 3013.
 - [26] Shore J.D., Holtzer M. and Sethna J.P., 1992, Phys. Rev. B **46**, 11376.
 - [27] Bouchaud J.P., Cugliandolo L.F., Kurchan J. and Mezard M., 1998 in *Spin Glasses and Random Fields*, edited by A.P. Young, World Scientific, Singapore.
 - [28] Bray A.J., 1994, *Adv. Phys.* **43**, 357.
 - [29] Sherrington D. and Kirkpatrick S., 1975, Phys. Rev. Lett. **35**, 1972.
 - [30] Bonilla L.L., Padilla F.G., and Ritort F., 1998, Physica A **250**, 315.
 - [31] Fisher D.S. and Huse D.A., 1998, Phys. Rev. B **38**, 386.
 - [32] See <http://www.lassp.cornell.edu/sethna/Coarsening/>
 - [33] Lifshitz I.M. and Slyozov V.V., 1961, J. Phys. Chem. Solids **19**, 35.
 - [34] Lifshitz I.M., 1962, Zh. Eksp. Teor. Fiz. **42**, 1354.
 - [35] Allen S.M. and Cahn J.W., 1979, Acta. Metall. **27**, 1085.
 - [36] Derrida B., 1997, Phys. Rev. E **55**, 3705.
 - [37] Hinrichen H. and Antoni M., 1998, Phys. Rev. E **75**, 2650.
 - [38] Oitmaa J., 1981, J. Phys. A **14**, 1159.
 - [39] Cirillo E.N.M., Gonnella G. and Stramaglia S., 1999, Il Nouvo Cimento D **20**, Supp. December.
 - [40] Lipowski A. and Johnston D., 2000, Phys. Rev. E **61**, 6375.
 - [41] Viot P. and Tarjus G., 1998, Europhys. Lett. **44**, 423.
 - [42] Grousson M., Tarjus G. and Viot P., 2002, Phys. Rev. E **65**, 065103.
 - [43] Berg B.A., 1998, Nucl. Phys. B (Proc. Suppl.) **63** A-C, 982.